

## SUPPORTING INFORMATION

### Highly-grafted Polystyrene/Polyvinylpyridine polymer gold nanoparticles in good solvent: effect of chain length and composition

Zbyšek Posel,<sup>a,b,\*</sup> Paola Posocco,<sup>c,d,\*</sup> Martin Lísal,<sup>b,e</sup> Maurizio Fermeglia<sup>c,d</sup> and Sabrina  
Pricl<sup>c,d\*</sup>

<sup>a</sup>Department of Informatics, Faculty of Science, J. E. Purkinje University,  
Ústí nad Labem, Czech Republic

<sup>b</sup>Laboratory of Physics and Chemistry of Aerosols, Institute of Chemical Process  
Fundamentals of the CAS, v. v. i., Prague, Czech Republic

<sup>c</sup>Molecular Simulations Engineering (MOSE) Laboratory, Department of Engineering and  
Architecture (DEA), University of Trieste, via Valerio 10, 34127 Trieste, Italy

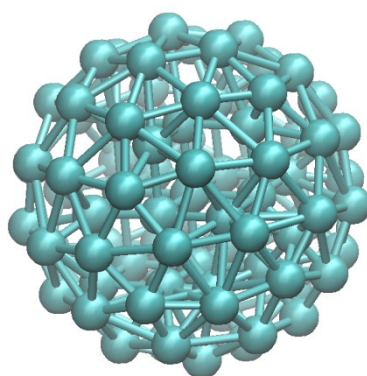
<sup>d</sup>National Interuniversity Consortium for Material Science and Technology (INSTM),  
Research Unit MOSE-DEA, University of Trieste, Italy

<sup>e</sup>Department of Physics, Faculty of Science, J. E. Purkinje University,  
Ústí nad Labem, Czech Republic

### Table of Content

<b>Au nanoparticle model.....</b>	
<b>Additional simulation details.....</b>	
<b>Scaling behaviour of polymer grafted nanoparticles.....</b>	
<b>Statistics.....</b>	
<b>Additional results.....</b>	
<b>References.....</b>	

## Au nanoparticle model



Radius of sphere $r_s$ (DPD units)	1.06
Number of mesoscopic segments	85
Number of grafting sites	62
Density (DPD units)	6.0
Bonding radius $r_b$ (DPD units)	1.05

**Table SI 1** Mesoscopic model of spherical Au nanoparticle.

## Additional simulation details

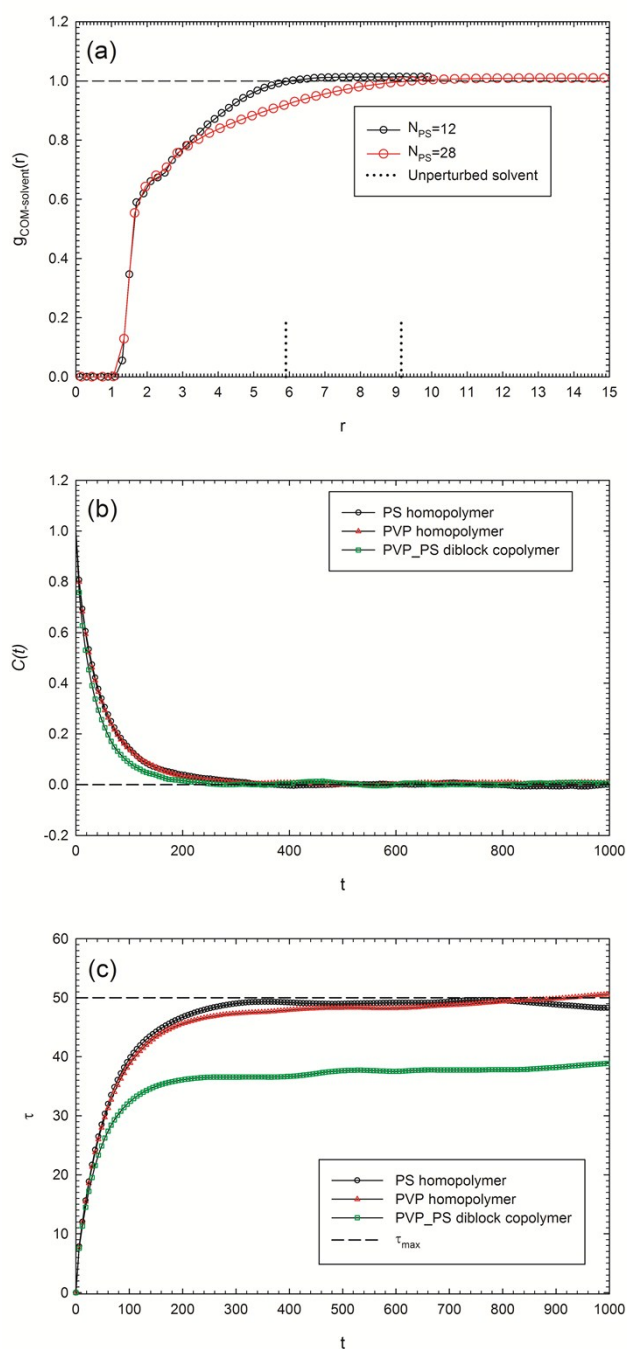


**Fig. SI 1** Dotted lines in Figure S1 a) show for two different poly(styrene) chain lengths the distance from the centre of mass of the nanoparticle at which the distribution of the solvent is unperturbed by polymer beads. Twice the size of this length was used to determine the simulation box length. (b) End-to-end distance correlation function  $C(t)$  and (c) correlation time  $\tau$  for the longest polymer chains in the simulation,  $N=28$ , used to estimate the interval between two stored configurations.

## Scaling behaviour of polymer grafted nanoparticles

If the size of a grafted chain exceeds the size of the nanoparticle and if the number of grafted chains  $G \gg 1$ , the scaling behaviour of polymer grafted nanoparticles can be described with the Daoud-Cotton (DC) model for star polymers<sup>1</sup>. Within the framework of the DC model single chain properties like end-to-end distance,  $R_e$ , and squared radius of gyration,  $R_g^2$ , scales as follows:

$$R_e \propto G^{(1-\nu)/2} N^\nu \approx G^{1/5} N^{3/5}$$

$$R_g^2 \propto G^{(1-\nu)} N^{2\nu} \approx G^{2/5} N^{6/5} \quad (\text{SI1})$$

The DC model predicts that each grafted polymer chain fills a conical sector that originates from the centre of mass of the nanoparticle and the free chain ends are placed only in the outer region of the polymer shell. Each polymer chains fill a conical sector up to brush height  $H$  that scales with the chain length  $N$  as:

$$H(N) \propto G^{(1-\nu)/2} N^\nu \approx G^{1/5} N^{3/5} \quad (\text{SI2})$$

We used the Flory exponent  $\nu=3/5$  for good solvent conditions on the right side of Eq.(SI1) and Eq. (SI2) for  $R_e$ ,  $R_g^2$  and  $H$ . Each conical sector contains at a distance  $r$  from the center of mass (COM) of the nanoparticle a certain constant number of polymer segments. Therefore, a region with high concentration of polymer segments is established near surface of the nanoparticle. In this inner region the exclude volume interactions are screened out and the monomer density profile scales as:

$$\phi(r) \approx \begin{cases} G^{1/2} r^{-1} & \text{inner region of corona} \\ G^{2/3} r^{-4/3} & \text{outer region of corona} \end{cases} \quad (\text{SI3})$$

At further distances from the COM of the nanoparticle the exclude volume effects, i.e. the interactions between polymer and solvent molecules, scales as  $G^{2/3} r^{-4/3}$ .

Mean end-to-end distance,  $R_e$ , and mean squared radius of gyration,  $R_g^2$ , were evaluated during simulation as:

$$R_e = \frac{1}{n} \left\langle \sum_{i=1}^n |\mathbf{r}_{1,i} - \mathbf{r}_{N,i}| \right\rangle$$

$$R_g^2 = \frac{1}{nN} \left\langle \sum_{i=1}^n \sum_{j=1}^N (\mathbf{r}_{j,i} - \mathbf{r}_{com,i})^2 \right\rangle$$
(SI4)

where  $n$  and  $N$  are the number of polymer chains in the system and total length of one polymer chain, respectively;  $\mathbf{r}_{com,i}$  is the position vector of the COM of the  $i$ -th chain and  $\mathbf{r}_{j,i}$  is the position vector of the  $j$ -th segment in the  $i$ -th chain.

Brush height was obtained from the end-monomer distribution  $\varphi(r)$  fitted to a Weibull distribution<sup>2</sup>

$$\Gamma(r) = a \left( \frac{d-1}{d} \right)^{\frac{1-d}{d}} \left[ \frac{r-r_{max}}{c} + \left( \frac{d-1}{d} \right)^{\frac{1}{d}} \right]^{d-1} \exp \left[ - \left( \frac{r-r_{max}}{c} + \left( \frac{d-1}{d} \right)^{\frac{1}{d}} \right)^d \frac{d-1}{d} \right]$$
(SI5)

where  $a$  is the amplitude,  $r$  is the distance from the COM of the nanoparticle,  $r_{max}$  is the position of maximum and  $d$  reflects the shape of the distribution. In Eq.(SI5) the brush height corresponds to  $r_{max}$ .

In order to obtain the scaling behaviour we fitted  $R_e$  and  $H$  using the following models:

$$R_e = H = \alpha G^{\frac{1-A}{2}} N^A$$
(SI6)

and  $R_g^2$  with

$$R_g^2 = \alpha G^{1-A} N^{2A}$$
(SI7)

where  $\alpha$  and  $A$  are scaling coefficients. Monomer density profiles were fitted in two regions separately. The inner region of the corona was fitted from the surface of the nanoparticle to the half size of the  $R_e$  of the grafted chains. The outer part was fitted from the half of the  $R_e$  to  $R_e$  of the grafted chains. Monomer density profile were fitted and reported in the corresponding graphs for the longest chain length (i.e.  $N = 28$ ).

## Statistics

The mean value of a variable  $O$  was calculated as the arithmetic mean  $\bar{O}$  averaged over all stored configurations as<sup>3</sup>

$$\bar{O} = \frac{1}{N_{run}} \sum_{i=1}^{N_{run}} O_i \quad (\text{SI8})$$

where  $N_{run}$  is total number of stored configurations. Since we expected uncorrelated configurations, the arithmetic mean substituted the ensemble average. Therefore, the time between two uncorrelated configurations  $\tau(t) = N_{samp} \Delta t$  was estimated in preliminary simulation runs for the systems with the longest chain length ( $N = 28$ ) as

$$\tau(t) = \frac{1}{2} + \sum_{k=1}^{N_{run}^p} C(k) \left( 1 - \frac{k}{N_{run}^p} \right) \quad (\text{SI9})$$

where  $C(t)$  is the correlation function,  $t = k * N_{samp} \Delta t$ ,  $N_{samp}$  is the interval between two stored configurations. The maximum correlation time  $\tau_{max}$  is typically estimated from the longest correlation function found in the studied systems. Since we were primarily interested in statistics involving chain behaviour we used the end-to-end distance  $R_e$  correlation function

$$C(t) = \frac{\langle \mathbf{R}_e(0) \cdot \mathbf{R}_e(t) \rangle}{\langle \mathbf{R}_e(0) \cdot \mathbf{R}_e(0) \rangle} \quad (\text{SI10})$$

All fluctuations that decay faster than  $\tau_{max}$  are excluded from the statistics. Therefore, the common practice is to reduce the interval of configuration storing by a factor  $k_r$ , since fluctuations can be relevant, for example, in observing the tendency of a variable. Then, the final interval of storing the configurations was calculated as

$$N_{samp} = \frac{\tau_{max}}{k_r \Delta t} \quad (\text{SI11})$$

Fig SI 1b) shows the end-to-end distance correlation function  $C(t)$  for PS and PVP homopolymers and for PVP-PS symmetric diblock copolymer chains grafted on spherical nanoparticles. Fig SI 1c) shows the corresponding correlation times  $\tau$  with the estimated maximum correlation time  $\tau_{max} = 50$ . From Eq.(SI11) we estimated the interval between two

stored configurations as  $N_{smp} = 200$  simulation steps with  $k_r=8$  and  $\Delta t=0.03$ . Accordingly, the storing interval together with the number of stored configurations  $N_{run}$  determined the total number of simulation steps as  $N_{simul} = N_{smp} * N_{run} = 2e^6$  simulation steps.

## Additional results

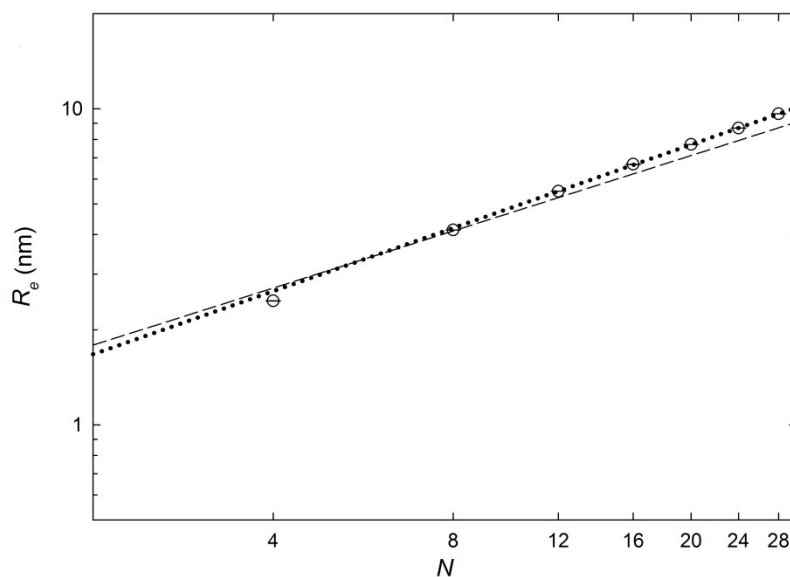


**Fig. SI 2** Log-log plot of the mean end-to-end distance  $R_e$  of PS homopolymer chains with different chain lengths  $N$  grafted onto spherical Au NPs. The dotted line represents the scaling of  $R_e$  obtained for long polymer chains (i.e.,  $N > 16$ ) while the dashed line shows the scaling of the Daoud-Cotton model.

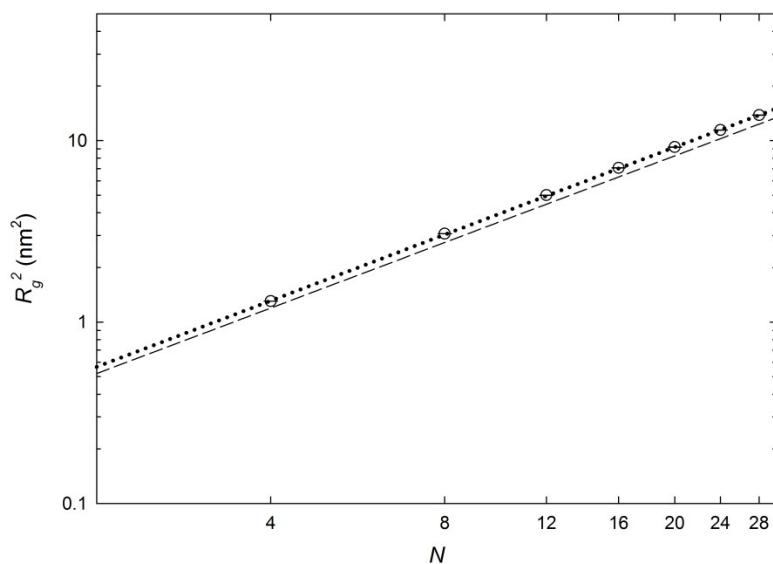


**Fig. SI 3** Log-log plot of the mean square radius of gyration  $R_g^2$  of PS homopolymer chains with different chain lengths  $N$  grafted onto spherical Au NPs. The dotted line represents the scaling of  $R_g^2$  obtained for long polymer chains (i.e.,  $N > 16$ ) while the dashed line shows the scaling of the Daoud-Cotton model.



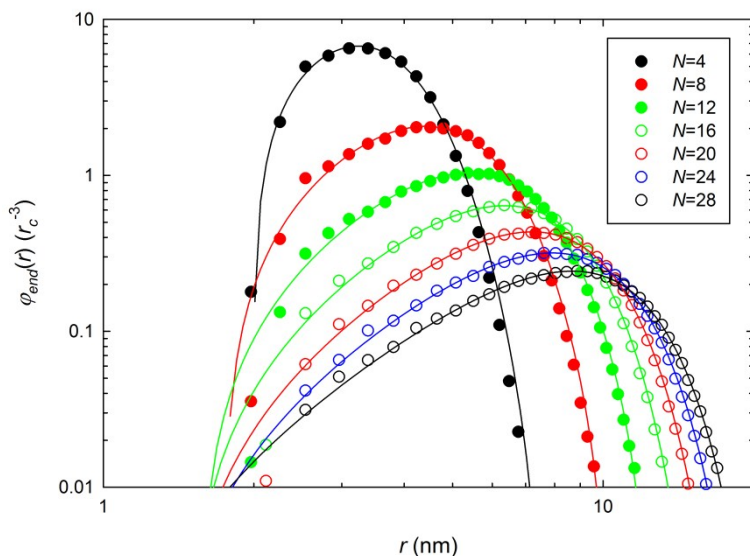


**Fig. SI 4** Log-log plot of end-monomer distribution  $\varphi_{end}(r)$  for PS homopolymer chains with different chain lengths  $N$  grafted onto Au NPS.  $\varphi_{end}(r)$  was fitted to the Weibull distribution and represented by a solid line.

**Table SI 2** Radius of gyration  $R_g$  of PS and PVP homopolymers and of symmetric  $PVP_nPS_n$  diblock copolymer grafted on the surface of Au spherical nanoparticles. Simulation uncertainties are given in the last digit as subscripts. The radius of the nanoparticle was fixed to  $r_s = 1.5$  nm.

Radius of gyration, $R_g$ (nm)							
$N$	4	8	12	16	20	24	28
PS	1.14 <sub>2</sub>	1.75 <sub>1</sub>	2.23 <sub>6</sub>	2.65 <sub>9</sub>	3.03 <sub>4</sub>	3.38 <sub>2</sub>	3.71 <sub>7</sub>
PVP	1.12 <sub>0</sub>	1.70 <sub>7</sub>	2.16 <sub>9</sub>	2.57 <sub>2</sub>	2.93 <sub>2</sub>	3.25 <sub>9</sub>	3.56 <sub>7</sub>
$PVP_nPS_n$	1.26 <sub>8</sub>	1.91 <sub>2</sub>	2.41 <sub>9</sub>	2.89 <sub>7</sub>	3.25 <sub>4</sub>	3.61 <sub>2</sub>	3.95 <sub>5</sub>

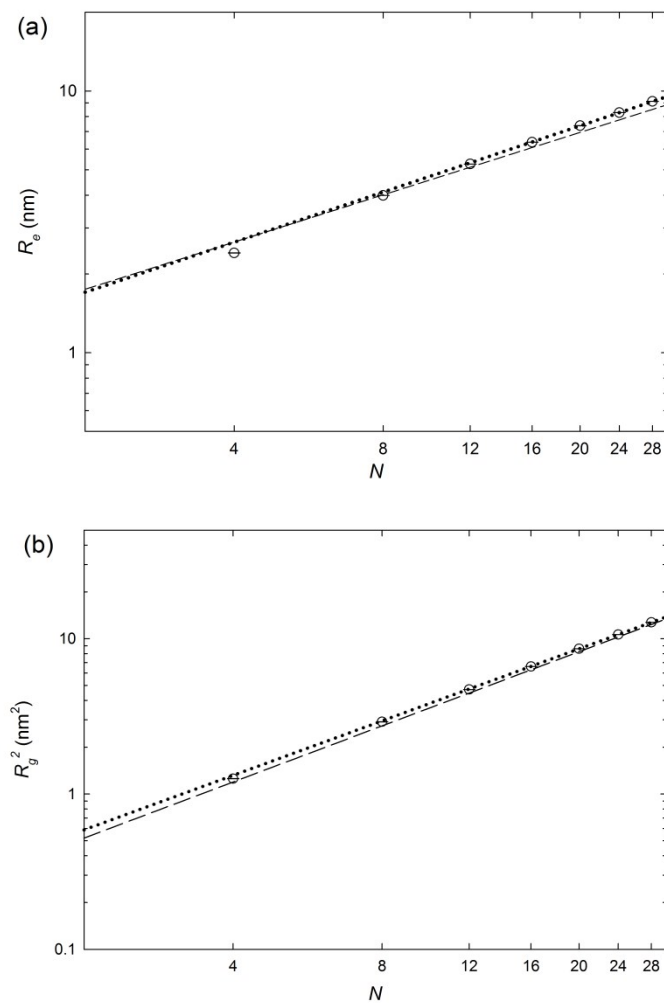


**Fig. SI 5** a) Mean end-to-end distance  $R_e$  and b) mean square radius of gyration  $R_g^2$  of PVP homopolymer chains with different chain lengths  $N$  plot in log-log scale. Dotted line represents scaling of  $R_e$  and  $R_g^2$ , obtained for long polymer chains (i.e.,  $N > 16$ ), and dashed line shows the scaling of the Daoud-Cotton model.

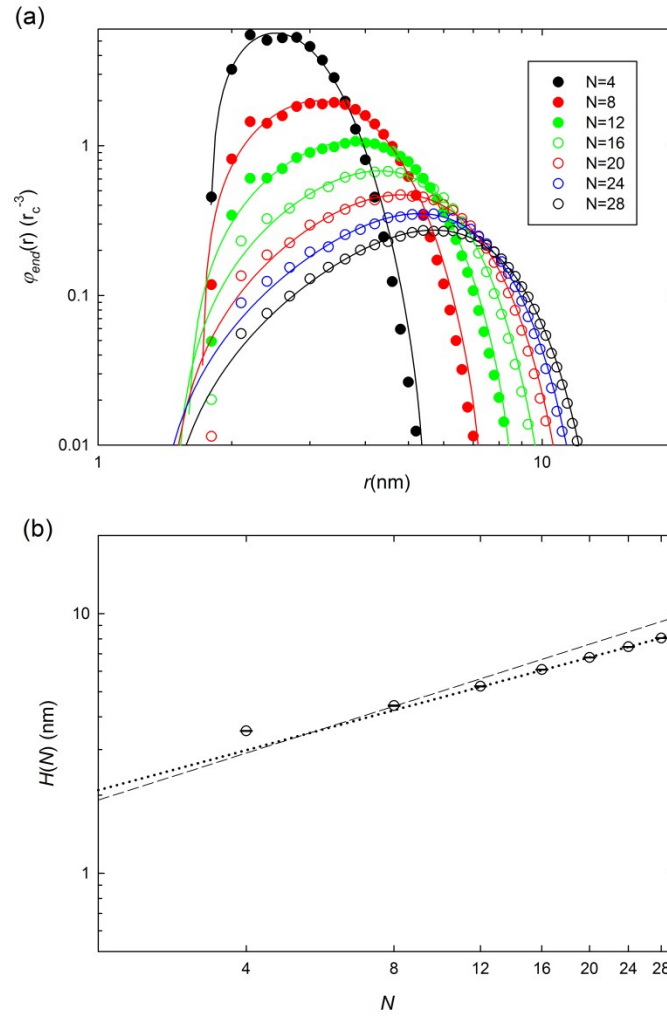


**Fig. SI 6** a) Log-log plot of end-monomer number distribution  $\phi_{end}(r)$  for PVP homopolymer chains with different chain lengths  $N$  measured from the center of mass of the nanoparticle.  $\phi_{end}(r)$  was fitted to a Weibull distribution and represented by a solid line. b) Brush height  $H(N)$  obtained as a maximum of a Weibull distribution for different chain lengths  $N$ . Dotted line represents the scaling of  $H(N)$ , plotted with the scaling of the Daoud-Cotton model in dashed line for comparison.

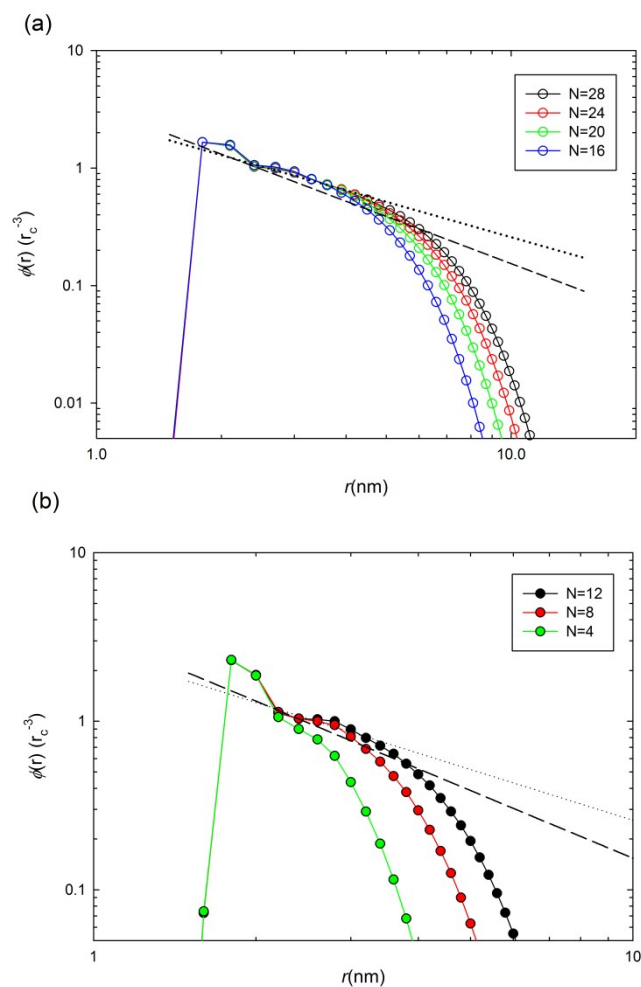


**Fig. SI 7** Log-log plot of monomer number density profiles  $\phi(r)$  measured from the center of mass of the nanoparticle. Solid line serves as a guide to the eye. a) Monomer density profiles  $\phi(r)$  for PVP homopolymer chains with  $N \geq 16$ . b) Monomer density profiles  $\phi(r)$  for short PVP homopolymer chains (i.e.,  $N < 16$ ). Dashed line represents scaling of the inner part of the profile, while dash-dotted line corresponds to the scaling of the outer part of the density profile. Scaling behavior was fitted for the longest chain in our simulation, i.e.  $N=28$ .

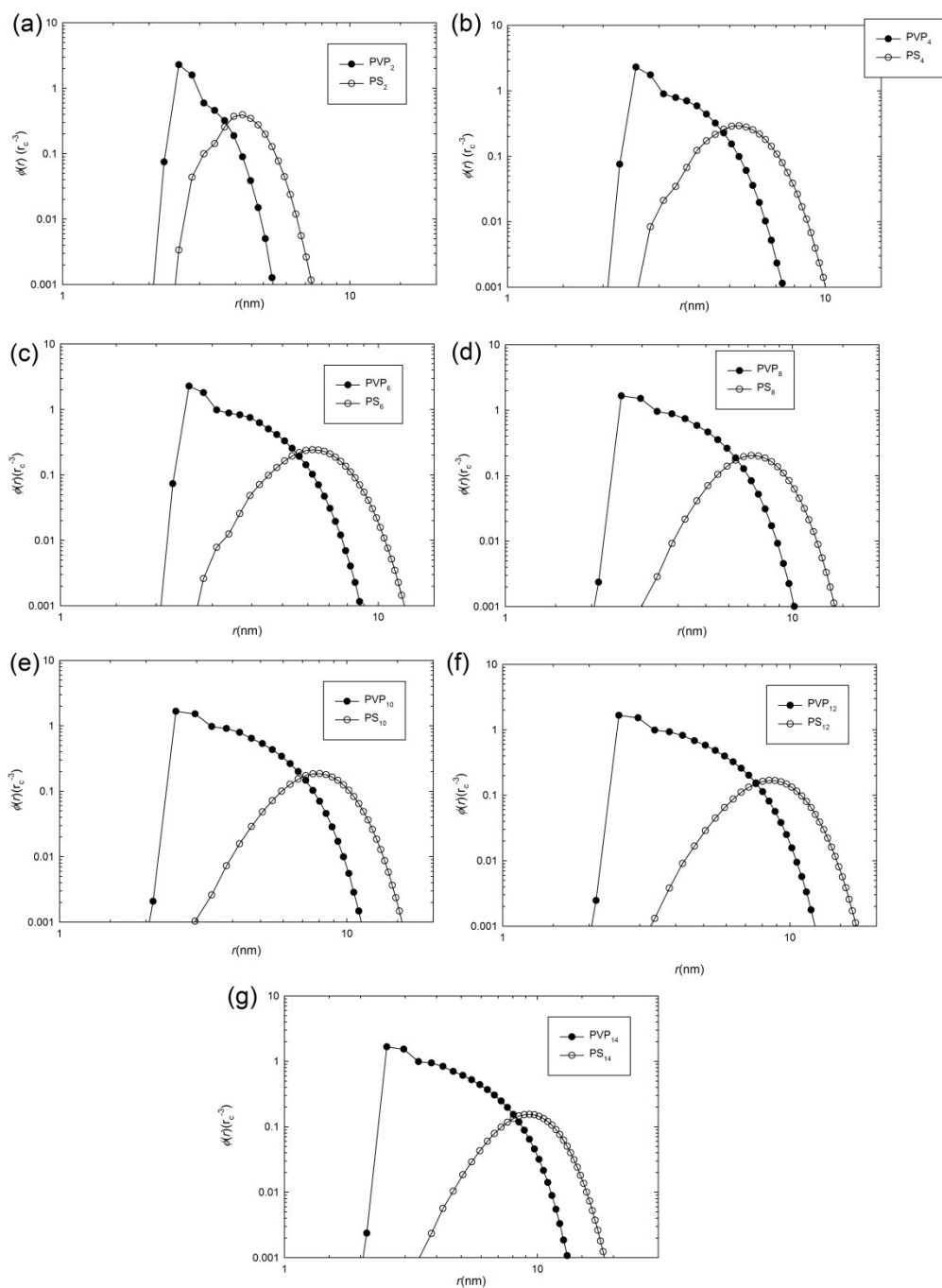


**Fig. SI 8** Log-log plot of monomer density profiles  $\phi(r)$  for (a) PVP<sub>2</sub>PS<sub>2</sub>, (b) PVP<sub>4</sub>PS<sub>4</sub>, (c) PVP<sub>6</sub>PS<sub>6</sub>, (d) PVP<sub>8</sub>PS<sub>8</sub>, (e) PVP<sub>10</sub>PS<sub>10</sub>, (f) PVP<sub>12</sub>PS<sub>12</sub> and (g) PVP<sub>14</sub>PS<sub>14</sub> symmetric DBC chain. Full circles show density profiles of PVP<sub>n</sub> beads and empty symbols show PS<sub>n</sub> beads.

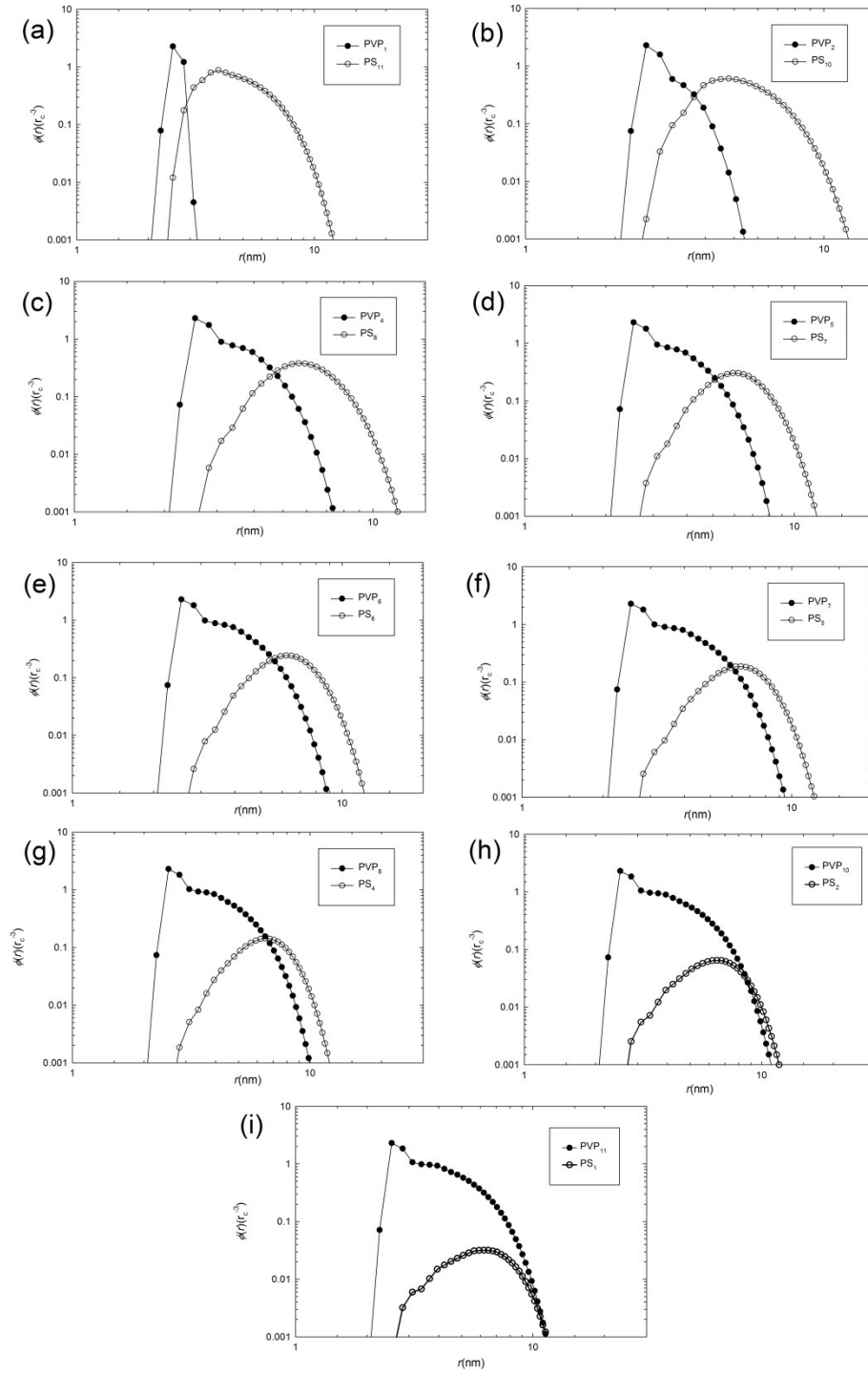


**Fig. SI 9** Log-log plot of monomer density profiles  $\phi(r)$  for DBC chain with  $N = n + m = 12$ . (a) PVP<sub>1</sub>PS<sub>11</sub>, (b) PVP<sub>2</sub>PS<sub>10</sub>, (c) PVP<sub>4</sub>PS<sub>8</sub>, (d) PVP<sub>5</sub>PS<sub>7</sub>, (e) PVP<sub>6</sub>PS<sub>6</sub>, (f) PVP<sub>7</sub>PS<sub>5</sub>, (g) PVP<sub>8</sub>PS<sub>4</sub>, (h) PVP<sub>10</sub>PS<sub>2</sub> and (i) PVP<sub>11</sub>PS<sub>1</sub>. Full circles show density profiles of PVP<sub>m</sub> beads and empty symbols show PS<sub>n</sub> beads.

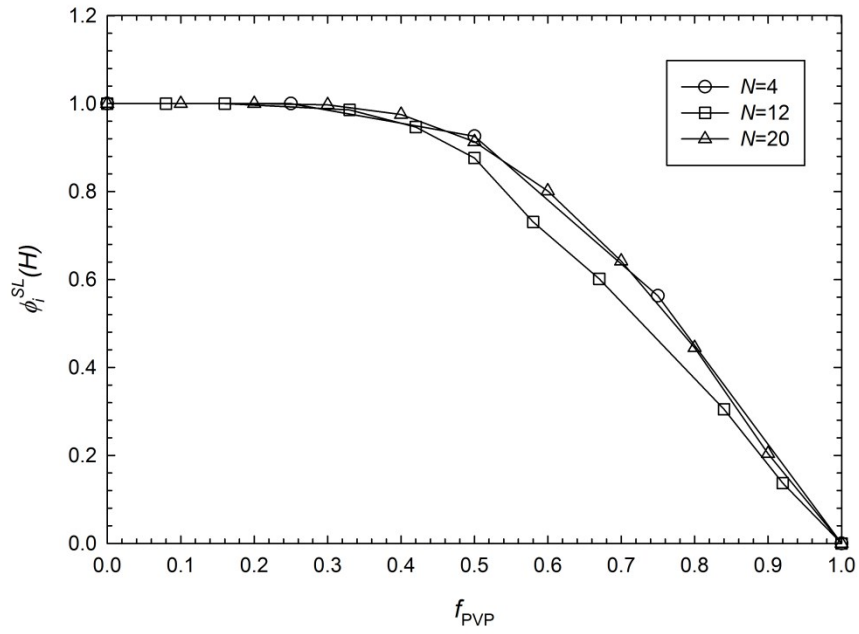


**Fig. SI 10** Effect of the chain architecture ( $f_{PVP}$ ) on the composition,  $\phi_i^{SL}$  of the surface layer for DBC chain with  $N = 4, 12$  and  $20$ . Data are plotted for PS beads only.

In an attempt to elucidate the effect of the repulsion parameter between PVP<sub>m</sub> and PS<sub>n</sub> block (and, in turn, of the monomer/particle interactions) on the surface layer, two different simulation scenarios were considered as reported in Figure SI 11. In the first case, the repulsion between PVP<sub>m</sub> and PS<sub>n</sub> block was taken into account (full and empty circles, value of  $a_{PS-PVP}$  reported in Table 3 of the main text). Then, in the second virtual scenario no additional repulsion between PVP and PS beads (full and empty triangles and dashed line,  $a_{PS-PVP}=25.0$ ) was considered. When the repulsion is switched on the breakeven point is observed around  $f_{PVP}=0.72$  and around  $f_{PVP}=0.69$  when the repulsion is switched off. Such small shift of breakeven point may indicate that additional repulsion does not play a major role in formation and composition of surface layer.

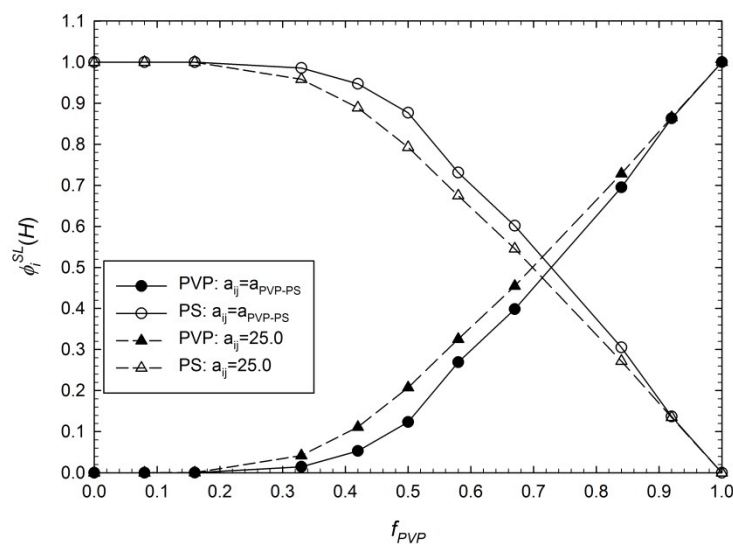


**Fig. SI 11** Effect of the architecture ( $f_{PVP}$ ) on the surface layer composition  $\phi_i^{SL}$  of a DBC of total length  $N = 12$ . Two simulation scenarios were considered. In first scenario (solid line) the repulsive interaction between PVP<sub>m</sub> and PS<sub>n</sub> block was taken into account, while in second scenario (dashed line) the repulsion was virtually switched off.



## References

- 1) M. Daoud and J. P. Cotton, *J. Physique*, 1982, **43**, 531-538.
- 2) W. Weibull, *J. Appl. Mech.-Trans. ASME* **18** (3), 293–297.
- 3) Janke W., John von Neumann Institute for Computing, Jülich, NIC Series, 2002, **10**, 423 – 445.